
AlignIQL: Policy Alignment in Implicit Q-Learning through Constrained Optimization

Longxiang He

Center for Artificial Intelligence and Robotics
Tsinghua University
hlx22@mails.tsinghua.edu.cn

Li Shen

Sun Yat-Sen University
shenli6@mail.sysu.edu.cn
shenli6@mail.sysu.edu.cn

Junbo Tan

Center for Artificial Intelligence and Robotics
Tsinghua University
tjblql@sz.tsinghua.edu.cn

Xueqian Wang

Center for Artificial Intelligence and Robotics
Tsinghua University
wang.xq@sz.tsinghua.edu.cn

Abstract

Implicit Q-learning (IQL) serves as a strong baseline for offline RL, which learns the value function using only dataset actions through quantile regression. However, it is unclear how to recover the implicit policy from the learned implicit Q-function and why IQL can utilize weighted regression for policy extraction. IDQL reinterprets IQL as an actor-critic method and gets weights of implicit policy, however, this weight only holds for the optimal value function. In this work, we introduce a different way to solve the *implicit policy-finding problem* (IPF) by formulating this problem as an optimization problem. Based on this optimization problem, we further propose two practical algorithms AlignIQL and AlignIQL-hard, which inherit the advantages of decoupling actor from critic in IQL and provide insights into why IQL can use weighted regression for policy extraction. Compared with IQL and IDQL, we find our method keeps the simplicity of IQL and solves the implicit policy-finding problem. Experimental results on D4RL datasets show that our method achieves competitive or superior results compared with other SOTA offline RL methods. Especially in complex sparse reward tasks like Antmaze and Adroit, our method outperforms IQL and IDQL by a significant margin. Code is available at <https://github.com/felix-thu/AlignIQL.git>

1 Introduction

Offline Reinforcement Learning (RL), or Batch RL aims to seek an optimal policy without environmental interactions [11, 26]. This is compelling for having the potential to transform large-scale datasets into powerful decision-making tools and avoids costly and risky online environmental interactions, which offers significant application prospects in fields such as healthcare [34, 46] and autopilot [50, 40]. Notwithstanding its promise, applying off-policy RL algorithms [28, 10, 12, 13] directly into the offline context presents challenges due to out-of-distribution actions that arise when evaluating the learned policy.[11, 26].

Despite a variety of methods based on constraint and conservative Q-learning have been proposed to address this, IQL [23] stands out among them since IQL avoids query out-of-distribution (OOD) actions entirely and decouples the critic from the actor, which contributes to stability and hyperparameter robust. However, IQL extracts policy through advantage-weighted regression (AWR) [32, 36, 38], resulting in the inconsistency between the extracted policy and the implicit policy in the learned Q-function. To solve this problem, IDQL [14] reinterprets IQL as an actor-critic method and derives

the implicit optimal policy weights. Nevertheless, this optimal weight hinges on the assumption that the optimal value function can be learned through parametrization (e.g. neural networks) and certain critic loss functions. It remains unclear whether extracting implicit policy with AWR is feasible and what is the policy implied by an arbitrary value function. Moreover, many recent offline RL [4] and safe RL methods [51] use IQL to learn the Q-function. Addressing these issues can lead to a better understanding of the bottlenecks of IQL-style methods, thereby promoting the development of offline RL.

In this paper, we solve this problem by formulating the policy-finding problem as an optimization problem, where the objective function is a generalized form of behavior regularizers and the constraint is policy alignment, which ensures the learned policy is the policy implied in the value function. By solving this optimization problem, we can get a closed-form solution, which can be expressed by imposing weight on the behavior policy. The weight can be computed by a value function, an action-value function, and multipliers. This weight shows that using AWR for policy extraction in IQL is feasible when the certain multiplier < 0 . Furthermore, our work explains how the implicit policy in IQL-style methods addresses OOD actions from the perspective of behavior regularizers.

Based on the optimization problem, we further propose two practical algorithms, AlignIQL-hard and AlignIQL. Both inherit the characteristics of IQL, namely the decoupling of actor and critic training and implicitly trained value function while achieving policy alignment. AlignIQL-hard can theoretically achieve a globally optimal solution, but it is more vulnerable to hyperparameter choices than AlignIQL. AlignIQL is simpler to implement and performs better in complex tasks like sparse rewards tasks, but it does not guarantee convergence to the global optimum.

Since behavior policy is often complex and potentially multi-modal, the unimodal Gaussian policy used with IQL is unlikely to accurately approximate the complex behavior policy [47, 14, 5, 16], which in turn affects the implicit policy extraction, as the general form of implicit policy is $\pi(\mathbf{s}|\mathbf{a}) \propto \mu(\mathbf{a}|\mathbf{s})w(\mathbf{s}, \mathbf{a})$, where $\mu(\mathbf{a}|\mathbf{s})$ is the behavior policy. We, therefore, use the diffusion model [41, 17, 43] to model the behavior policy. For policy extraction, we select actions from a diffusion-parameterized behavior model with weights derived from our policy-finding problem, which enjoy both superior expressivity and policy alignment. We verify the effectiveness of AlignIQL on D4RL datasets and demonstrate the state-of-the-art performance, especially on sparse reward datasets in which the critic learning is hard and unstable. We also show that, compared to IDQL, AlignIQL is more robust to hyperparameters and achieves more stable training.

To summarize, our main contributions are as follows:

- We propose the policy-finding problem, where the policy alignment term is added as a constraint. By solving this problem, we provide insights into why and when IQL can use weighted regression for policy extraction, and in turn, make it better to understand the bottlenecks of the IQL-style algorithms.
- We demonstrate that there is no price to achieving policy alignment in IQL-style methods, all we need is to modify the importance weights of the policy extraction based on the sign of multiplier or hyperparameter η . These results can be generalized to any generalized value loss function, which greatly extends the theoretical results of IDQL.
- We introduce two practical IQL-style algorithms: AlignIQL-hard and AlignIQL, which obtain competitive performance on D4RL datasets and show robustness on sparse reward tasks. Extensive experiments, together with the theoretical analysis, validate the effectiveness of our proposed approaches.

2 Background

Offline RL. Consider a Markov decision process (MDP): $M = \{\mathcal{S}, \mathcal{A}, P, R, \gamma, d_0\}$, with state space \mathcal{S} , action space \mathcal{A} , environment dynamics $\mathcal{P}(\mathbf{s}'|\mathbf{s}, \mathbf{a}) : \mathcal{S} \times \mathcal{S} \times \mathcal{A} \rightarrow [0, 1]$, reward function $R : \mathcal{S} \times \mathcal{A} \rightarrow \mathbb{R}$, discount factor $\gamma \in [0, 1]$, policy $\pi(\mathbf{a}|\mathbf{s}) : \mathcal{S} \times \mathcal{A} \rightarrow [0, 1]$, and initial state distribution d_0 . The action-value or Q-value of policy π is defined as $Q^\pi(\mathbf{s}_t, \mathbf{a}_t) = \mathbb{E}_{\mathbf{a}_{t+1}, \mathbf{a}_{t+2}, \dots \sim \pi} \left[\sum_{j=0}^{\infty} \gamma^j r(\mathbf{s}_{t+j}, \mathbf{a}_{t+j}) \right]$. The goal of RL is to get a policy to maximize the cumulative discounted reward $J(\theta) = \int_{\mathcal{S}} d_0(\mathbf{s}) Q^\pi(\mathbf{s}, \mathbf{a}) d\mathbf{s}$. $d^\pi(\mathbf{s}) = \sum_{t=0}^{\infty} \gamma^t p_\pi(\mathbf{s}_t = \mathbf{s})$ is the state visitation distribution induced by policy π [45, 37], and $p_\pi(\mathbf{s}_t = \mathbf{s})$ is the likelihood of the policy

being in state s after following π for t timesteps. In offline setting [11], environmental interaction is not allowed, and a static dataset $\mathcal{D} \triangleq \{(\mathcal{S}, \mathcal{A}, R, S', \text{done})\}$ is used to learn a policy.

Implicit Q-learning (IQL). To avoid OOD actions in offline RL, IQL [22] uses the state conditional upper expectile of action-value function $Q(s, \mathbf{a})$ to estimate the value function $V(s)$, which avoid directly querying a Q-function with unseen action. For a parameterized critic $Q_\theta(s, \mathbf{a})$, target critic $Q_{\hat{\theta}}(s, \mathbf{a})$, and value network $V_\psi(s)$ the value objective is learned by

$$\begin{aligned} \mathcal{L}_V(\psi) &= \mathbb{E}_{(s, \mathbf{a}) \sim \mathcal{D}} [L_2^\tau(Q_{\hat{\theta}}(s, \mathbf{a}) - V_\psi(s))] \\ \text{where } L_2^\tau(u) &= |\tau - \mathbb{1}(u < 0)|u^2, \end{aligned} \quad (1)$$

where $\mathbb{1}$ is the indicator function. Then, the Q-function is learned by minimizing the MSE loss

$$\mathcal{L}_Q(\theta) = \mathbb{E}_{(s, \mathbf{a}, s') \sim \mathcal{D}} [(r(s, \mathbf{a}) + \gamma V_\psi(s') - Q_\theta(s, \mathbf{a}))^2]. \quad (2)$$

Note that, in IQL, the corresponding policy is not explicitly represented, it is implicit in the learned value function. For policy extraction, IQL uses AWR [39, 37, 33]

$$\mathcal{L}_\pi(\phi) = \mathbb{E}_{(s, \mathbf{a}) \sim \mathcal{D}} [\exp(\alpha(Q_{\hat{\theta}}(s, \mathbf{a}) - V_\psi(s))) \log \pi_\phi(\mathbf{a}|s)]. \quad (3)$$

Implicit Diffusion Q-learning (IDQL). To find the implicit policy in the learned value function, IDQL [14] generalizes the value loss in Equation 1 with an arbitrary convex loss U on the difference $Q - V$.

$$V^*(s) = \arg \min_{V(s)} \mathbb{E}_{\mathbf{a} \sim \mu(\mathbf{a}|s)} [U(Q(s, \mathbf{a}) - V(s))] = \arg \min_{V(s)} \mathcal{L}_V^U(V(s)). \quad (4)$$

Under some assumptions about U , IDQL derives the implicit policy in optimal V defined in Equation 4

$$w(s, \mathbf{a}) = \frac{|U'(Q(s, \mathbf{a}) - V^*(s))|}{|Q(s, \mathbf{a}) - V^*(s)|}, \quad (5)$$

which yields an expression for the implicit actor as $\pi_{\text{imp}}(\mathbf{a}|s) \propto \mu(\mathbf{a}|s)w(s, \mathbf{a})$.

However, it remains unclear whether it is feasible to extract policy with AWR. Answering this question can help us better understand the bottlenecks of IQL-style methods. Before drawing our conclusion, we first introduce the form of our Implicit Policy-finding Problem.

3 Implicit Policy-finding Problem

Before introducing the implicit policy-finding problem, we first introduce Definition 3.1, which defines what a policy implied by a value function $Q(s, \mathbf{a})$ is.

Definition 3.1. We refer to a policy as one implied by the value function $Q(s, \mathbf{a}), V(s)$, when

$$Q(s, \mathbf{a}) - r(s, \mathbf{a}) - \gamma \mathbb{E}_{s' \sim p(s'|s, \mathbf{a}), \mathbf{a}' \sim \pi(\mathbf{a}|s)} [Q(s', \mathbf{a}')] = 0. \quad (6)$$

$$\mathbb{E}_{\mathbf{a} \sim \pi(\mathbf{a}|s)} [Q(s, \mathbf{a})] = V(s), \quad (7)$$

Definition 3.1 is derived from IDQL [14] and the conventional definition of the value function in actor-critic methods. Note that in IQL, the Q-function is updated by minimizing Equation 2, which implies if we can ensure Equation 7, Equation 6 can be derived by substituting Equation 7 back in Equation 2. So in IQL, we can define the implicit policy when it satisfies Equation 7.

It is known that the offline RL problem can be solved by constrained policy search (CPS) problem (aka AWR) [32, 36, 38], where a policy is sought to maximize cumulative rewards under the constraint of policy divergence from the behavior policy. (See more details in Appendix C) Inspired by CPS, we formulate the *implicit policy-finding problem* (IPF) as a constrained optimization, where a policy is sought to minimize policy divergence from the behavior policy under policy alignment

$$\begin{aligned} \min_{\pi} \quad & \mathbb{E}_{s \sim d^\pi(s), \mathbf{a} \sim \pi(\mathbf{a}|s)} \left[f \left(\frac{\pi(\mathbf{a}|s)}{\mu(\mathbf{a}|s)} \right) \right] \\ \text{s.t.} \quad & \pi(\mathbf{a}|s) \geq 0, \quad \forall s, \forall \mathbf{a} \\ & \int_{\mathbf{a}} \pi(\mathbf{a}|s) d\mathbf{a} = 1, \quad \forall s \\ & \mathbb{E}_{\mathbf{a} \sim \pi(\mathbf{a}|s)} [Q(s, \mathbf{a})] - V(s) = 0, \quad \forall s, \end{aligned} \quad (\text{IPF})$$

where $V(\mathbf{s}), Q(\mathbf{s}, \mathbf{a})$ is the learned value function, which does not have to be the optimal value function. $f(\cdot)$ is a regularization function which aims to avoid out-of-distribution actions. The third constraint ensures that the learned policy is the policy implied in Q, V .

Here we briefly describe the characteristics of the solution to problem IPF. In Problem IPF, when the feasible set includes multiple policies (*i.e.* multiple implicit policies satisfy Definition 3.1), problem IPF aims to find an optimal implicit policy that deviates least from the behavior policy while satisfying the requirements of policy alignment. In other cases, when the feasible set has a unique policy, problem IPF will return the unique policy as the optimal implicit policy. The above analysis shows that we can model the implicit policy-finding problem in IQL as problem IPF.

Assumption 3.2. Assume $\pi(\mathbf{a}|\mathbf{s}) > 0 \implies \mu(\mathbf{a}|\mathbf{s}) > 0$ so that $\frac{\pi(\mathbf{a}|\mathbf{s})}{\mu(\mathbf{a}|\mathbf{s})}$ is well-defined. [49]

Assumption 3.3. Assume that $f(x)$ is differentiable on $(0, \infty)$ and that $h_f(x) = xf(x)$ is strictly convex and $f(1) = 0$. [49]

Remark 3.4. Under the above assumptions, problem IPF is a convex optimization problem and assumption 3.3 makes the regularization term positive due to Jensen’s inequality as $\mathbb{E}_\mu[\frac{\pi}{\mu} f(\frac{\pi}{\mu})] \geq 1f(1) = 0$ [49]. Slater’s conditions hold since constraint 1 and constraint 2 define a probability simplex, and constraint 3 defines a hyperplane in the tabular setting. The intersection of these convex sets is nonempty if the optimal policy exists, *i.e.* the optimal policy is not a uniform distribution. The analysis described above shows that this convex optimization problem is feasible and Slater’s conditions are satisfied.

4 Optimization

In this section, we introduce two methods AlignIQL-hard and AlignIQL for solving problem IPF. Theoretically, AlignIQL-hard is more rigorous as it strictly ensures policy alignment and provides insights into why IQL can use AWR for policy extraction, but it suffers from complex training. AlignIQL avoids the training complexity of AlignIQL-hard while also guaranteeing local convergence to the optimal solution of problem IPF through soft constraints. All proof can be found in Appendix A

4.1 AlignIQL-hard

We first consider directly solving IPF with KKT conditions and get the following theorems.

Theorem 4.1. For problem IPF, the optimal policy π^* and its optimal Lagrange multipliers satisfy the following optimality condition for all states and actions:

$$\pi^*(\mathbf{a}|\mathbf{s}) = \mu(\mathbf{a}|\mathbf{s}) \max \{g_f(-\alpha^*(\mathbf{s}) - \beta^*(\mathbf{s})Q(\mathbf{s}, \mathbf{a})), 0\}. \quad (8)$$

$$\mathbb{E}_{\mathbf{a} \sim \mu} [\max \{g_f(-\alpha^*(\mathbf{s}) - \beta^*(\mathbf{s})Q(\mathbf{s}, \mathbf{a})), 0\}] = 1, \quad (9)$$

$$\mathbb{E}_{\mathbf{a} \sim \mu(\mathbf{a}|\mathbf{s})} [Q(\mathbf{s}, \mathbf{a}) \max \{g_f(-\alpha^*(\mathbf{s}) - \beta^*(\mathbf{s})Q(\mathbf{s}, \mathbf{a})), 0\} - V(\mathbf{s})] = 0, \quad (10)$$

where α^*, β^* is the Lagrange multiplier, g_f is the inverse function of $h_f(x)$.

Remark 4.2. Note that α^* is a normalization term, it does not affect the action generated by the policy. Let $f(x) = \log x$, then $g_f(x) = \exp(x - 1) > 0$, we can get $\pi^*(\mathbf{a}|\mathbf{s}) \propto \mu(\mathbf{a}|\mathbf{s}) \exp(-\beta^*Q(\mathbf{s}, \mathbf{a}))$. In most environments (especially MuJoCo tasks), β^* we learned through the neural network is negative. Because only the positive and negative of β^* affect the action generated by the policy, we can approximate β^* with a fixed $\beta \in (0, \infty]$, *i.e.* $\pi^*(\mathbf{a}|\mathbf{s}) \propto \mu(\mathbf{a}|\mathbf{s}) \exp(\beta Q(\mathbf{s}, \mathbf{a}))$, which is exactly what optimal policy obtained by AWR. This explains why IQL can learn implicit policy with weighted regression and shows implicit policy avoids the OOD actions through the regularization function f , which gives a deeper understanding of how IQL-style methods handle the distribution shift. This also addresses the issue in IDQL, that is, they find that simply taking the action with the highest Q-value tends to yield better performance at evaluation time.

Although implicit policy can be extracted by Equation 8, how to handle weights is a key issue for IQL, especially when we use the diffusion model to approximate the behavior policy. Because we use the importance sampling weights to select actions from learned behavior policy. The weight used in prior works is an increasing function of $Q(\mathbf{s}, \mathbf{a})$, however according to Theorem 4.1, when $\beta^*(\mathbf{s}) \geq 0$, we need to be more conservative, that is, we should choose actions with lower $Q(\mathbf{s}, \mathbf{a})$. To calculate the weights, we need to solve the closed-form solution of Equation 9, Equation 10, which is usually intractable. However, we can resort to the parameterized neural network to approximate solve it.

Algorithm 1 AlignIQL Training	Algorithm 2 AlignIQL Policy Extraction
1: Initialize behavior policy network μ_ϕ , critic networks Q_θ, V_ψ , and target networks $\mu_{\hat{\phi}}, Q_{\hat{\theta}}$, multiplier networks $\alpha_\omega(\mathbf{s}), \beta_\chi(\mathbf{s})$	1: Pretraining: $Q_{\hat{\theta}}, V_\psi, \mu_\phi$, multiplier networks $\alpha_\omega(\mathbf{s}), \beta_\chi(\mathbf{s})$
2: for $t = 1$ to T do	2: Samples per state N, η
3: Sample from $\mathcal{B} = \{(\mathbf{s}_t, \mathbf{a}_t, r_t, \mathbf{s}_{t+1})\} \sim \mathcal{D}$.	3: while not done do
4: # Critic updating	4: Get current state \mathbf{s}
5: $\psi \leftarrow \psi - \lambda \nabla_\psi \mathcal{L}_V(\psi)$ (Equation 1)	5: Sample $a_i \sim \mu_\phi(\mathbf{a} \mathbf{s}), i = 1, \dots, N$
6: $\theta \leftarrow \theta - \lambda \nabla_\theta \mathcal{L}_Q(\theta)$ (Equation 2)	6: if AlignIQL-hard: then
7: if AlignIQL-hard: then	7: Compute weight $w(\mathbf{s}, \mathbf{a})$ through Equation 8
8: # Multiplier network updating	8: else
9: $\omega \leftarrow \omega + \lambda \nabla_\omega \mathcal{L}_M(\omega)$	9: Compute weight $w(\mathbf{s}, \mathbf{a})$ through Equation 12
10: $\chi \leftarrow \chi + \lambda \nabla_\chi \mathcal{L}_M(\chi)$	10: end if
11: end if	11: Normalize: $p_i = \frac{w(\mathbf{s}, a_i)}{\sum_j w(\mathbf{s}, a_j)}$
12: $\phi \leftarrow \phi - \lambda \nabla_\phi \mathcal{L}_\mu(\phi)$ (Equation 41)	12: Select a_{taken} with the highest probability according to p_i
13: # Target Networks updating	13: end while
14: $\hat{\theta} \leftarrow (1 - \eta)\hat{\theta} + \eta\theta$	
15: end for	

Lemma 4.3. *Following EQL [49], let $f(x) = \log x$, then $g_f(x) = \exp(x - 1) > 0$. We can approximate $\alpha^*(\mathbf{s}), \beta^*(\mathbf{s})$ through neural network with the following loss function:*

$$\max_{\alpha, \beta} \mathcal{L}_M = -\mathbb{E}_{\mathbf{a} \sim \mu} [\exp(-\alpha(\mathbf{s}) - \beta(\mathbf{s})Q(\mathbf{s}, \mathbf{a}) - 1)] - \alpha(\mathbf{s}) - \beta(\mathbf{s})V(\mathbf{s}), \quad (11)$$

Proof. Then Lemma 4.3 can be get through setting the gradient of Equation 11 to 0 with respect to α, β , which is Equation 9, Equation 10 respectively. \square

Remark 4.4. Now we can obtain α^*, β^* by iteratively updating α, β following Equation 11.

Based on Theorem A.1 and Lemma 4.3, we can get a practical algorithm AlignIQL-hard, where hard means we rigidly constrain the policy to satisfy policy alignment. AlignIQL-hard shows when multiplier $\beta(\mathbf{s}) < 0$, we can use AWR for extracting the implicit policy in IQL. However, for strict policy alignment, AlignIQL-hard needs to train an additional two multiplier networks, which increases the training costs and compound errors. Moreover, the exponential term in Equation 11 makes the unstable training. In the remainder of this section, we introduce a more simple and effective method AlignIQL to solve problem IPF.

4.2 AlignIQL

In this section, we introduce AlignIQL to solve the alignment problem of IQL. Firstly, we introduce the soft constraint form of problem IPF. Given $\eta \in \mathbb{R} \setminus 0$, IPF-Soft is defined as

$$\begin{aligned} \min_{\pi, V(\mathbf{s})} \quad & \mathbb{E}_{\mathbf{s} \sim d^\pi(\mathbf{s}), \mathbf{a} \sim \pi(\mathbf{a}|\mathbf{s})} \left[f \left(\frac{\pi(\mathbf{a}|\mathbf{s})}{\mu(\mathbf{a}|\mathbf{s})} \right) + \eta (Q(\mathbf{s}, \mathbf{a}) - V(\mathbf{s}))^2 \right] \\ \text{s.t.} \quad & \pi(\mathbf{a}|\mathbf{s}) \geq 0, \quad \forall \mathbf{s}, \forall \mathbf{a} \\ & \int_{\mathbf{a}} \pi(\mathbf{a}|\mathbf{s}) d\mathbf{a} = 1, \quad \forall \mathbf{s}. \end{aligned} \quad (\text{IPF-Soft})$$

Remark 4.5. We refer to the above problem as problem IPF-Soft, since it does not rigidly keep the policy alignment. But we will show problem IPF-Soft approximately solves problem IPF through Proposition 4.8. More importantly, in practice, AlignIQL does not require training multiplier networks, making the training more stable, efficient, and resulting in better performance.

Theorem 4.6. *Suppose that $f(x) = \log x$, then the optimal policy of problem IPF-Soft satisfies*

$$\pi^*(\mathbf{a}|\mathbf{s}) \propto \exp \left\{ -\eta (Q(\mathbf{s}, \mathbf{a}) - V(\mathbf{s}))^2 \right\}. \quad (12)$$

Remark 4.7. Equation 12 and Equation 8 are very similar, but the difference is that Equation 12 extract policy based on η rather than multiplier $\beta(\mathbf{s})$, which avoids training the multiplier network. For

$\eta > 0$, Equation 12 prefers actions that minimize $(Q(\mathbf{s}, \mathbf{a}) - V(\mathbf{s}))^2$. For $\eta < 0$, Equation 12 prefers actions that maximize the absolute value of the advantage function $|A(\mathbf{s}, \mathbf{a})| = |Q(\mathbf{s}, \mathbf{a}) - V(\mathbf{s})|$. However, the absolute function can not distinguish between positive and negative values. To solve this problem, we suppose that the probabilities of $A(\mathbf{s}, \mathbf{s}) > 0$ and $A(\mathbf{s}, \mathbf{s}) < 0$ for the sampled actions are equal and choose actions with $A(\mathbf{s}, \mathbf{a}) > 0$ since $A(\mathbf{s}, \mathbf{a}) \geq 0$ means better actions, that is, for $\eta < 0$, we use the $w(\mathbf{s}, \mathbf{a}) \propto \exp\{|\eta|(Q(\mathbf{s}, \mathbf{a}) - V(\mathbf{s}))\}$ as the weight. Note that in this case, $w(\mathbf{s}, \mathbf{a})$ is actually the same as the weight used by IQL, SfBC [5] and it is very similar to the w_{exp} of IDQL. This demonstrates the connection between IQL-style algorithms and Weighted Regression.

Next, we show the relationship between problem IPF and problem IPF-Soft.

Proposition 4.8. *Suppose that $\pi^*(\mathbf{a}|\mathbf{s})$ is a global solution to the convex optimization problem IPF, with its corresponding value function (denoted as $V^*(\mathbf{s})$). Then $\pi^*, V^*(\mathbf{s})$ is a strict local minimizer of problem IPF-Soft for all*

$$\eta(h^* - k^*) < 0,$$

where $h^* = \mathbb{E}_{\mathbf{a} \sim \pi^*} [(Q(\mathbf{s}, \mathbf{a}) - V^*(\mathbf{s}))^2]$, $k^* = \inf_{\pi \in \mathcal{T}} \mathbb{E}_{\mathbf{a} \sim \pi} [(Q(\mathbf{s}, \mathbf{a}) - V(\mathbf{s}))^2]$,

$$\mathcal{T} = \left\{ \pi | \pi(\mathbf{a}|\mathbf{s}) \geq 0, \int_{\mathbf{a}} \pi(\mathbf{a}|\mathbf{s}) d\mathbf{a} = 1, V(\mathbf{s}) = \mathbb{E}_{\mathbf{a} \sim \pi(\mathbf{a}|\mathbf{s})} [Q(\mathbf{s}, \mathbf{a})], \pi \in \dot{U}(\pi^*, \sigma) \right\}.$$

Remark 4.9. Note that problem IPF-Soft may not be a convex optimization problem, as the objective function may not be a convex function. Through Proposition 4.8, solution of problem IPF can be found by approximately solving the problem IPF-Soft.

Note that in both AlignIQL-hard and AlignIQL, we do not impose a limit on the loss function of the $Q - V$, which means that our conclusion can be generalized to the arbitrary critic loss function and the arbitrary value function. To summarize, both the AlignIQL-hard and AlignIQL are IQL-style algorithms, which means the training of actor and critic are decoupled and the critic is learned by expectile regression. The difference between AlignIQL-hard and AlignIQL lies in the calculation of weights and the necessity of training multiplier networks. We summarize the procedure of AlignIQL-hard and AlignIQL in Algorithm 1 and Algorithm 2.

5 Experiments

In this section, we conduct extensive experiments and specifically answer the following questions

- **Q1:** Can AlignIQL match the performance with other SOTA offline RL baselines?
- **Q2:** Can AlignIQL derive any benefits from the alignment?
- **Q3:** Both IDQL and AlignIQL derive the weights needed for policy alignment. Are our weights better than IDQL?

5.1 Results on D4RL Tasks (Q1)

We conduct extensive experiments on D4RL datasets [9] to verify the performance of AlignIQL. For the selection of baselines, we select Conservative Q-learning (CQL) [25], DiffusionQL [47], Implicit-Q Learning (IQL) [22], SQL [49], SfBC [5] because of their strong performance in the offline RL setting. We also select the DD [1] and Diffuser [19] as baselines since they represent sequential-modeling-based RL algorithms. Aggregated results can be found in Table 1. In MuJoCo tasks, where the performance is already saturated, AlignIQL shows slightly worse results compared to the other methods. Since the performance in MuJoCo tasks is already saturated, the effect of policy alignment is not evident. However, in more challenging AntMaze tasks, AlignIQL outperforms other methods by a large margin. Above all, results in Table 1 show that AlignIQL can match the SOTA performance in MuJoCo tasks and achieve SOTA results in AntMaze tasks. More importantly, we find that compared to IDQL, AlignIQL is less sensitive to hyperparameter N . We will elaborate on this in the following sections. We include learning curves and experiment details in Appendix E to ensure the reproducibility of our results in Table 1.

5.2 The Role of Policy Alignment (Q2)

In this section, we conduct a detailed comparison of the impact of the sign of η in AlignIQL. According to Theorem A.2, the sign of η determines what policy the learned value function is actually

Table 1: The performance of our method and other SOTA baselines on D4RL tasks. The performance of AlignIQL and IDQL is obtained by evaluating the trained policy over 10 different random seeds. We report the performance of baseline methods using the best results reported from their papers except for IDQL. We rerun the official code of IDQL and report the results on the same hardware (RTX 4090 with 24GB memory) for a fair comparison. We report the result of AlignIQL and IDQL by taking the average of the last evaluation over 10 seeds. Results within 3% of the maximum in every D4RL task and the best average result are highlighted in SkyBlue.

Dataset	Environment	CQL	Diffusion-QL	SfBC	SQL	DD	Diffuser	IDQL	IQL	AlignIQL (ours)
Medium-Expert	HalfCheetah	62.4	96.8	92.6	94.0	90.6	79.8	89.2	86.7	89.1
Medium-Expert	Hopper	98.7	111.1	108.6	111.8	111.8	107.2	108.2	91.5	107.1
Medium-Expert	Walker2d	111.0	110.1	109.8	110.0	108.8	108.4	111.7	109.6	111.9
Medium	HalfCheetah	44.4	51.1	45.9	48.3	49.1	44.2	46.0	47.4	46.0
Medium	Hopper	58.0	90.5	57.1	75.5	79.3	58.5	56.3	66.3	56.1
Medium	Walker2d	79.2	87.0	77.9	84.2	82.5	79.7	77.6	78.3	78.5
Medium-Replay	HalfCheetah	46.2	47.8	37.1	44.8	39.3	42.2	41.1	44.2	41.1
Medium-Replay	Hopper	48.6	101.3	86.2	99.7	100.0	96.8	86.2	94.7	74.8
Medium-Replay	Walker2d	26.7	95.5	65.1	81.2	75.0	61.2	85.1	73.9	76.5
Average (Locomotion)		63.9	87.9	75.6	83.3	81.8	75.3	78.0	76.9	75.7
Default	AntMaze-umaze	74.0	93.4	92.0	92.2	-	-	93.4	87.5	94.8
Diverse	AntMaze-umaze	84.0	66.2	85.3	74.0	-	-	75.2	62.2	82.4
Play	AntMaze-medium	61.2	76.6	81.3	80.2	-	-	85	71.2	80.5
Diverse	AntMaze-medium	53.7	78.6	82.0	79.1	-	-	74.4	70.0	85.5
Play	AntMaze-large	15.8	46.4	59.3	53.2	-	-	60.0	39.6	65.2
Diverse	AntMaze-large	14.9	57.3	45.5	52.3	-	-	58.4	47.5	66.4
Average (AntMaze)		50.6	69.8	74.2	-	-	-	74.4	63.0	79.1
# Diffusion steps		-	5	15	-	100	100	5	-	5

evaluating. If $\eta = 1$ represents the aligned policy, then $\eta = -1$ corresponds to the misaligned policy and vice versa. Note that, when $\eta = -1$, the weight is equivalent to the weight of AWR, which selects actions based on the Q-function and is widely used in offline RL [5, 23, 14]. We choose the AntMaze tasks since challenging tasks can better show the effect of alignment. In the experiment shown in Figure 1, we use a diffusion-based behavior policy and guarantee that all the hyperparameters and network structures are the same except for η , which is used for policy alignment.

Figure 1 shows that under the same N (where N represents the samples per state), The correctly aligned policy ($\eta = 1$ in Figure 1) converges faster and does not experience a significant performance drop at higher $N = 256$. Generally, the greedy selection of actions based on Q-values [2, 13], which usually yields better results, performed poorly here. This is due to policy misalignment, leading to AWR-based weights assigning high values to out-of-distribution actions potentially generated by the behavior policy. In MuJoCo tasks, due to the relative simplicity of the tasks, the Q-function can achieve good generalization performance through training, so this issue is not pronounced.

Above all, the results in Figure 1 show the benefits of policy alignment and demonstrate the correctness of our theory through the performance difference of different η .

5.3 Comparison with IDQL (Q3)

Since both IDQL and AlignIQL provide weights under policy alignment, in this part we evaluate which weights are better through D4RL sparse reward tasks Adroit and ablation study on N . In the experiments in this section, both IDQL and AlignIQL use expectile regression to learn the critic and employ greedy extraction $\mathbf{a}_{\text{taken}} = \arg \max_{\mathbf{a}} w(\mathbf{s}, \mathbf{a})$ during evaluation. We use expectile regression to train critic since the expectile objective performs the strongest with greedy extraction as mentioned in IDQL. Of course, our AlignIQL framework can also be extended to other generalized critic loss functions mentioned in IDQL.

Results on D4RL Sparse Reward Tasks. We conduct the experiment on Adroit tasks. Compared with MuJoCo tasks, the Adroit tasks are high dimensional and feature sparse rewards. For human and expert datasets, the data is collected in from human demonstrators. Results can be found in Table 2. Table 2 shows that compared to IDQL, AlignIQL can achieve competitive results and significantly outperform IDQL on some challenging tasks like relocate-human.

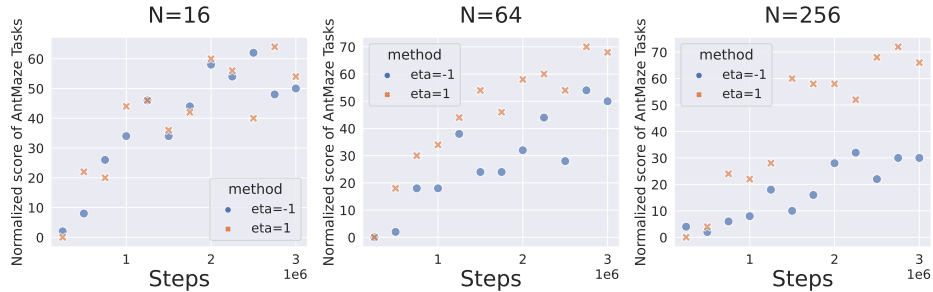


Figure 1: Performance of different η in AlignIQL on AntMaze tasks with different training steps. The horizontal axis represents time (s) on a logarithmic scale. Results are averaged over 10 random seeds.

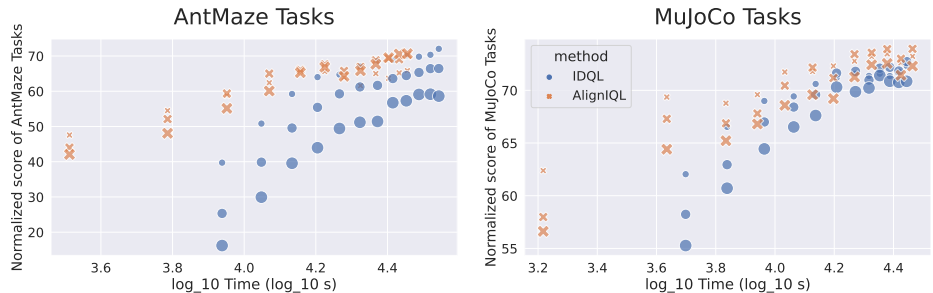


Figure 2: Performance of AlignIQL and IDQL on AntMaze tasks with different training steps. The different sizes, from smallest to largest, represent $N = 16$, $N = 64$, $N = 256$, respectively.

Ablation Study. Since the main limitation of diffusion-based methods is the running speed, we compare the performance of IDQL and AlignIQL at different training times in Figure 2. Figure 2 shows that as training time increases, the performance of AlignIQL with different N converges to the same value, which shows that AlignIQL is insensitive to N . We also observe that AlignIQL converges faster compared to IDQL.

Overall, compared to IDQL, the weights computed by our method not only have better theoretical properties (applicable to any Q-loss, without requiring optimal V) but also perform better in practice.

Table 2: Normalized scores of AlignIQL against other baselines on D4RL sparse-reward tasks. We **bold** the mean values that $\geq 0.99 * \text{highest value}$. “-A” refers to we only sweep over $\eta \in \{-1, 1\}$ while keeping other parameters the same as the IDQL. AlignIQL refers to we fix $\eta = 1$.

Task	BC	BCQ	CQL	IQL	AlignIQL-A	Algae-DICE	IDQL	AlignIQL
pen-human	63.9	68.9	37.5	71.5	76.0 ± 4.8	-3.3	70.7 ± 8.4	76.0 ± 4.8
hammer-human	1.2	0.5	4.4	1.4	2.7 ± 1.2	0.3	2.8 ± 0.8	2.0 ± 0.7
door-human	2.0	0.0	9.9	4.3	7.3 ± 4.9	0.0	5.2 ± 1.3	6.0 ± 3.6
relocate-human	0.1	-0.1	0.2	0.1	0.3 ± 0.1	-0.1	0.09 ± 0.02	0.28 ± 0.34
pen-expert	85.1	114.9	107.0	111.7	139.2 ± 6.5	-3.5	132.9 ± 4.5	116.0 ± 4.3
hammer-expert	125.6	107.2	86.7	116.3	124.7 ± 1.9	0.3	126.5 ± 0.7	124.7 ± 1.9
door-expert	34.9	99.0	101.5	103.8	105.2 ± 0.2	0.0	105.0 ± 0.1	104.6 ± 0.5
relocate-expert	101.3	41.6	95.0	102.7	107.7 ± 2.7	-0.1	108.3 ± 1.3	106.0 ± 1.5

6 Related Work

Offline RL. Offline RL algorithms need to avoid OOD actions. Previous methods to mitigate this issue under the model-free offline RL setting generally fall into three categories: 1) value function-based approaches, which implement pessimistic value estimation by assigning low scores

to out-of-distribution actions [25, 11], or implicit TD backups [24, 31] to avoid the use of out-of-distribution actions 2) sequential modeling approaches, which casts offline RL as a sequence generation task with return guidance [6, 19, 27, 1], and 3) constrained policy search (CPS) approaches, which regularizes the discrepancy between the learned policy and behavior policy [39, 37, 33].

Implicit Q-learning. Recently, *implicit Q-learning* [24] has attracted interest due to its stable training and simplicity. Many offline RL methods [4, 51, 14] use IQL-style expectile regression to learn Q-function and realize the advantage of decoupling the training of actor and critic. While IQL achieves superior performance, several issues remain unsolved. SQL [49] reinterprets IQL in the Implicit Value Regularization (IVR) framework and provides insights about why in practice a large τ may give a worse result in IQL. However, there is another important open question about IQL, that is, what policy the learned value function is evaluating. IDQL [14] solves this by reinterpreting the IQL as an actor-critic method and getting the corresponding implicit policy for the (generalized) IQL loss function. However, the corresponding implicit policy in IDQL only holds for optimal value function under certain critic loss functions.

Diffusion Model in Offline RL. Due to our method using the diffusion model for modeling behavior policy, we review works that incorporate the Diffusion model in offline RL. There exist several works that introduce the diffusion model to RL. Diffuser [19] uses the diffusion model to directly generate trajectory guided with gradient guidance or reward. DiffusionQL [47] uses the diffusion model as an actor and optimizes it through the TD3+BC-style objective with a coefficient η to balance the two terms. AdaptDiffuser [27] uses a diffusion model to generate extra trajectories and a discriminator to select desired data to add to the training set to enhance the adaptability of the diffusion model. DD [1] uses a conditional diffusion model to generate trajectory and compose skills. Unlike Diffuser, DD diffuses only states and trains inverse dynamics to predict actions. QGPO [30] uses the energy function to guide the sampling process and proves that the proposed CEP training method can get an unbiased estimation of the gradient of the energy function under unlimited model capacity and data samples. IDQL [15] reinterpret IQL as an Actor-Critic method and extract the policy through sampling from a diffusion-parameterized behavior policy with weights computed from the IQL-style critic. EDP [20] focuses on boosting sampling speed through approximated actions. SRPO [4] uses a Gaussian policy in which the gradient is regularized by a pretrained diffusion model to recover the IQL-style policy. Our method is distinct from these methods because we aim to align the implied policy in the value function.

The closest work to ours is IDQL [14], which derives the implicit policy for optimal value function under different critic loss functions. Our method is related, but features with AlignIQL apply to arbitrary value functions and arbitrary critic loss functions. More importantly, our method explains when and why IQL can use AWR for policy extraction while providing theoretical insights for IQL and other RL paradigms that use Q-values to guide sampling.

7 Discussion and Future Work

In our work, we define the implicit policy-finding problem in IQL and propose two practical algorithms AlignIQL-hard and AlignIQL to solve it. The optimal policy (Theorem A.1) in AlignIQL-hard shows that it is feasible to extract policy with AWR in certain cases, which builds the bridge between the Implicit Q-learning and Weighted Regression. Our theoretical findings also extend the policy alignment of IDQL to arbitrary critic loss and value functions. Besides the theoretical findings, we also verify the effectiveness of our algorithm on D4RL datasets. Experimental results show that compared to other IQL-style algorithms, our algorithm achieves SOTA performance and is more stable, especially in sparse reward tasks. One future work is to explore better methods for training multiplier networks and explore the impact of different regularization functions of problem IPF. Another future work is to extend our approach to fields of safe RL and offline-to-online (O2O) learning. In safe RL, prior works [51, 3] have used IQL to learn the Q-function. Investigating how to ensure policy alignment while satisfying safety constraints is an interesting research direction.

Limitation. Our work focus on regularization function $f(x) = \log x$ due to its simplicity. However, different regularization functions can result in different type policy. For example, SQL [49] shows using $f(x) = x - 1$ can introduce sparsity in learning the state-value function. In future work, we can explore other regularization functions to obtain better policy.

Boarder Impact. Our method will promote the development of offline reinforcement learning, thus facilitating the implementation of offline reinforcement learning in practical scenarios, such as robotic control. Since our work primarily focuses on RL theory, it will not raise ethical issues.

References

- [1] Anurag Ajay, Yilun Du, Abhi Gupta, Joshua B Tenenbaum, Tommi S Jaakkola, and Pulkit Agrawal. Is conditional generative modeling all you need for decision making? In *The Eleventh International Conference on Learning Representations*, 2022.
- [2] David Brandfonbrener, William F. Whitney, Rajesh Ranganath, and Joan Bruna. Offline RL Without Off-Policy Evaluation, December 2021.
- [3] Chenyang Cao, Zichen Yan, Renhao Lu, Junbo Tan, and Xueqian Wang. Offline goal-conditioned reinforcement learning for safety-critical tasks with recovery policy. *arXiv preprint arXiv:2403.01734*, 2024.
- [4] Huayu Chen, Cheng Lu, Zhengyi Wang, Hang Su, and Jun Zhu. Score regularized policy optimization through diffusion behavior.
- [5] Huayu Chen, Cheng Lu, Chengyang Ying, Hang Su, and Jun Zhu. Offline reinforcement learning via high-fidelity generative behavior modeling. In *The Eleventh International Conference on Learning Representations*, 2022.
- [6] Lili Chen, Kevin Lu, Aravind Rajeswaran, Kimin Lee, Aditya Grover, Misha Laskin, Pieter Abbeel, Aravind Srinivas, and Igor Mordatch. Decision transformer: Reinforcement learning via sequence modeling. *Advances in neural information processing systems*, 34:15084–15097, 2021.
- [7] Xinyue Chen, Zijian Zhou, Zheng Wang, Che Wang, Yanqiu Wu, and Keith Ross. Bail: Best-action imitation learning for batch deep reinforcement learning. *Advances in Neural Information Processing Systems*, 33:18353–18363, 2020.
- [8] Prafulla Dhariwal and Alexander Nichol. Diffusion models beat gans on image synthesis. *Advances in neural information processing systems*, 34:8780–8794, 2021.
- [9] Justin Fu, Aviral Kumar, Ofir Nachum, George Tucker, and Sergey Levine. D4rl: Datasets for deep data-driven reinforcement learning. *arXiv preprint arXiv:2004.07219*, 2020.
- [10] Scott Fujimoto, Herke Hoof, and David Meger. Addressing function approximation error in actor-critic methods. In *International Conference on Machine Learning*, pages 1587–1596. PMLR, 2018.
- [11] Scott Fujimoto, David Meger, and Doina Precup. Off-policy deep reinforcement learning without exploration. In *International Conference on Machine Learning*, pages 2052–2062. PMLR, 2019.
- [12] Tuomas Haarnoja, Aurick Zhou, Pieter Abbeel, and Sergey Levine. Soft actor-critic: Off-policy maximum entropy deep reinforcement learning with a stochastic actor. In *International Conference on Machine Learning*, pages 1861–1870. PMLR, 2018.
- [13] Tuomas Haarnoja, Aurick Zhou, Kristian Hartikainen, George Tucker, Sehoon Ha, Jie Tan, Vikash Kumar, Henry Zhu, Abhishek Gupta, and Pieter Abbeel. Soft actor-critic algorithms and applications. *arXiv preprint arXiv:1812.05905*, 2018.
- [14] Philippe Hansen-Estruch, Ilya Kostrikov, Michael Janner, Jakub Grudzien Kuba, and Sergey Levine. IDQL: Implicit Q-Learning as an Actor-Critic Method with Diffusion Policies, April 2023.
- [15] Philippe Hansen-Estruch, Ilya Kostrikov, Michael Janner, Jakub Grudzien Kuba, and Sergey Levine. Idql: Implicit q-learning as an actor-critic method with diffusion policies. *arXiv preprint arXiv:2304.10573*, 2023.

- [16] Longxiang He, Li Shen, Linrui Zhang, Junbo Tan, and Xueqian Wang. Diffcops: Diffusion model based constrained policy search for offline reinforcement learning, 2024.
- [17] Jonathan Ho, Ajay Jain, and Pieter Abbeel. Denoising diffusion probabilistic models. *Advances in neural information processing systems*, 33:6840–6851, 2020.
- [18] Jonathan Ho and Tim Salimans. Classifier-free diffusion guidance. In *NeurIPS 2021 Workshop on Deep Generative Models and Downstream Applications*, 2021.
- [19] Michael Janner, Yilun Du, Joshua B. Tenenbaum, and Sergey Levine. Planning with diffusion for flexible behavior synthesis. *arXiv preprint arXiv:2205.09991*, 2022.
- [20] Bingyi Kang, Xiao Ma, Chao Du, Tianyu Pang, and Shuicheng Yan. Efficient diffusion policies for offline reinforcement learning. *Advances in Neural Information Processing Systems*, 36, 2024.
- [21] Diederik P Kingma and Jimmy Ba. Adam: A method for stochastic optimization. *arXiv preprint arXiv:1412.6980*, 2014.
- [22] Ilya Kostrikov, Rob Fergus, Jonathan Tompson, and Ofir Nachum. Offline reinforcement learning with fisher divergence critic regularization. In *International Conference on Machine Learning*, pages 5774–5783. PMLR, 2021.
- [23] Ilya Kostrikov, Ashvin Nair, and Sergey Levine. Offline Reinforcement Learning with Implicit Q-Learning, October 2021.
- [24] Ilya Kostrikov, Ashvin Nair, and Sergey Levine. Offline reinforcement learning with implicit q-learning. In *International Conference on Learning Representations*, 2021.
- [25] Aviral Kumar, Aurick Zhou, George Tucker, and Sergey Levine. Conservative q-learning for offline reinforcement learning. *Advances in Neural Information Processing Systems*, 33:1179–1191, 2020.
- [26] Sergey Levine, Aviral Kumar, George Tucker, and Justin Fu. Offline reinforcement learning: Tutorial, review, and perspectives on open problems. *arXiv preprint arXiv:2005.01643*, 2020.
- [27] Zhixuan Liang, Yao Mu, Mingyu Ding, Fei Ni, Masayoshi Tomizuka, and Ping Luo. Adaptdiffuser: Diffusion models as adaptive self-evolving planners. *arXiv preprint arXiv:2302.01877*, 2023.
- [28] Timothy P. Lillicrap, Jonathan J. Hunt, Alexander Pritzel, Nicolas Heess, Tom Erez, Yuval Tassa, David Silver, and Daan Wierstra. Continuous control with deep reinforcement learning. *arXiv preprint arXiv:1509.02971*, 2015.
- [29] Ilya Loshchilov and Frank Hutter. Sgdr: Stochastic gradient descent with warm restarts. *arXiv preprint arXiv:1608.03983*, 2016.
- [30] Cheng Lu, Huayu Chen, Jianfei Chen, Hang Su, Chongxuan Li, and Jun Zhu. Contrastive energy prediction for exact energy-guided diffusion sampling in offline reinforcement learning. *arXiv preprint arXiv:2304.12824*, 2023.
- [31] Xiaoteng Ma, Yiqin Yang, Hao Hu, Qihan Liu, Jun Yang, Chongjie Zhang, Qianchuan Zhao, and Bin Liang. Offline reinforcement learning with value-based episodic memory. *arXiv preprint arXiv:2110.09796*, 2021.
- [32] Ashvin Nair, Abhishek Gupta, Murtaza Dalal, and Sergey Levine. Awac: Accelerating online reinforcement learning with offline datasets.
- [33] Ashvin Nair, Abhishek Gupta, Murtaza Dalal, and Sergey Levine. Awac: Accelerating online reinforcement learning with offline datasets. *arXiv preprint arXiv:2006.09359*, 2020.
- [34] Xinkun Nie, Emma Brunskill, and Stefan Wager. Learning when-to-treat policies. *Journal of the American Statistical Association*, 116(533):392–409, 2021.

- [35] Tim Pearce, Tabish Rashid, Anssi Kanervisto, Dave Bignell, Mingfei Sun, Raluca Georgescu, Sergio Valcarcel Macua, Shan Zheng Tan, Ida Momennejad, Katja Hofmann, et al. Imitating human behaviour with diffusion models. *arXiv preprint arXiv:2301.10677*, 2023.
- [36] Xue Bin Peng, Aviral Kumar, Grace Zhang, and Sergey Levine. Advantage-weighted regression: Simple and scalable off-policy reinforcement learning.
- [37] Xue Bin Peng, Aviral Kumar, Grace Zhang, and Sergey Levine. Advantage-weighted regression: Simple and scalable off-policy reinforcement learning. *arXiv preprint arXiv:1910.00177*, 2019.
- [38] Jan Peters, Katharina Mulling, and Yasemin Altun. Relative entropy policy search. In *Proceedings of the AAAI Conference on Artificial Intelligence*, volume 24, pages 1607–1612, 2010.
- [39] Jan Peters, Katharina Mulling, and Yasemin Altun. Relative entropy policy search. In *Proceedings of the AAAI Conference on Artificial Intelligence*, volume 24, pages 1607–1612, 2010.
- [40] Nicholas Rhinehart, Rowan McAllister, and Sergey Levine. Deep imitative models for flexible inference, planning, and control. *arXiv preprint arXiv:1810.06544*, 2018.
- [41] Jascha Sohl-Dickstein, Eric Weiss, Niru Maheswaranathan, and Surya Ganguli. Deep unsupervised learning using nonequilibrium thermodynamics. In *International Conference on Machine Learning*, pages 2256–2265. PMLR, 2015.
- [42] Kihyuk Sohn, Honglak Lee, and Xinchen Yan. Learning structured output representation using deep conditional generative models. *Advances in neural information processing systems*, 28, 2015.
- [43] Yang Song and Stefano Ermon. Generative modeling by estimating gradients of the data distribution. *Advances in neural information processing systems*, 32, 2019.
- [44] Yang Song, Jascha Sohl-Dickstein, Diederik P Kingma, Abhishek Kumar, Stefano Ermon, and Ben Poole. Score-based generative modeling through stochastic differential equations. *arXiv preprint arXiv:2011.13456*, 2020.
- [45] Richard S. Sutton and Andrew G. Barto. *Reinforcement Learning: An Introduction*. MIT press, 2018.
- [46] Huan-Hsin Tseng, Yi Luo, Sunan Cui, Jen-Tzung Chien, Randall K Ten Haken, and Issam El Naqa. Deep reinforcement learning for automated radiation adaptation in lung cancer. *Medical physics*, 44(12):6690–6705, 2017.
- [47] Zhendong Wang, Jonathan J. Hunt, and Mingyuan Zhou. Diffusion policies as an expressive policy class for offline reinforcement learning. *arXiv preprint arXiv:2208.06193*, 2022.
- [48] Ziyu Wang, Alexander Novikov, Konrad Zolna, Josh S. Merel, Jost Tobias Springenberg, Scott E. Reed, Bobak Shahriari, Noah Siegel, Caglar Gulcehre, and Nicolas Heess. Critic regularized regression. *Advances in Neural Information Processing Systems*, 33:7768–7778, 2020.
- [49] Haoran Xu, Li Jiang, Jianxiong Li, Zhuoran Yang, Zhaoran Wang, Victor Wai Kin Chan, and Xianyuan Zhan. Offline RL with No OOD Actions: In-Sample Learning via Implicit Value Regularization, March 2023.
- [50] Ekim Yurtsever, Jacob Lambert, Alexander Carballo, and Kazuya Takeda. A survey of autonomous driving: Common practices and emerging technologies. *IEEE access*, 8:58443–58469, 2020.
- [51] Yinan Zheng, Jianxiong Li, Dongjie Yu, Yujie Yang, Shengbo Eben Li, Xianyuan Zhan, and Jingjing Liu. Feasibility-guided safe offline reinforcement learning. In *The Twelfth International Conference on Learning Representations*, 2023.

A Proof

A.1 Proof of Theorem 3.4

Proof. The Lagrange function of Equation IPF is written as follows

$$\begin{aligned} L(\pi, \alpha(\mathbf{s}), \beta(\mathbf{s}), \lambda) &= \mathbb{E}_{\mathbf{s} \sim d^\pi(\mathbf{s}), \mathbf{a} \sim \pi(\mathbf{a}|\mathbf{s})} \left[f\left(\frac{\pi(\mathbf{a}|\mathbf{s})}{\mu(\mathbf{a}|\mathbf{s})}\right) \right] - \mathbb{E}_{\mathbf{s} \sim d^\pi(\mathbf{s}), \mathbf{a} \sim \pi(\mathbf{a}|\mathbf{s})} [\lambda(\mathbf{a}|\mathbf{s})\pi(\mathbf{a}|\mathbf{s})] \\ &\quad + \mathbb{E}_{\mathbf{s} \sim d^\pi(\mathbf{s})} \left[\alpha(\mathbf{s}) \left(\int_{\mathbf{a}} \pi(\mathbf{a}|\mathbf{s}) d\mathbf{a} - 1 \right) \right] + \\ &\quad \mathbb{E}_{\mathbf{s} \sim d^\pi(\mathbf{s})} [\beta(\mathbf{s}) (\mathbb{E}_{\mathbf{a} \sim \pi(\mathbf{a}|\mathbf{s})} [Q(\mathbf{s}, \mathbf{a})] - V(\mathbf{s}))], \end{aligned} \quad (13)$$

where $d^\pi(\mathbf{s})$ represents the state distribution induced by policy π , $\alpha(\mathbf{s})$, $\beta(\mathbf{s})$, and λ are Lagrangian multipliers for the equality and inequality constraints respectively.

Let $h_f(x) = xf(x)$. Then for all states and actions, the KKT conditions can be written as follows

$$\pi(\mathbf{a}|\mathbf{s}) \geq 0 \quad (14)$$

$$\int_{\mathbf{a}} \pi(\mathbf{a}|\mathbf{s}) d\mathbf{a} = 1 \quad (15)$$

$$\mathbb{E}_{\mathbf{a} \sim \pi(\mathbf{a}|\mathbf{s})} [Q(\mathbf{s}, \mathbf{a}) - V(\mathbf{s})] = 0 \quad (16)$$

$$\lambda(\mathbf{a}|\mathbf{s}) \geq 0 \quad (17)$$

$$\lambda(\mathbf{a}|\mathbf{s})\pi(\mathbf{a}|\mathbf{s}) = 0 \quad (18)$$

$$h'_f\left(\frac{\pi(\mathbf{a}|\mathbf{s})}{\mu(\mathbf{a}|\mathbf{s})}\right) + \alpha(\mathbf{s}) + \beta(\mathbf{s})Q(\mathbf{s}, \mathbf{a}) - \lambda(\mathbf{a}|\mathbf{s}) = 0 \quad (19)$$

We eliminate $d^\pi(\mathbf{s})$ due to irreducible Markov chain assumption. Note that in our derivation, we assume that $V(\mathbf{s})$ and $Q(\mathbf{s}, \mathbf{a})$ are known.

Since h'_f is a strictly increasing function, its inverse function exists and is also a strictly increasing function. Let $g_f = (h'_f)^{-1}(x)$ be its inverse function. From Equation 19, we can get

$$\pi(\mathbf{a}|\mathbf{s}) = \mu(\mathbf{a}|\mathbf{s})g_f(\lambda(\mathbf{a}|\mathbf{s}) - \alpha(\mathbf{s}) - \beta(\mathbf{s})Q(\mathbf{s}, \mathbf{a})) \quad (20)$$

Given a state \mathbf{s} , we can get $\lambda(\mathbf{a}|\mathbf{s}) = h'_f\left(\frac{\pi}{\mu}\right) + \alpha(\mathbf{s}) + \beta(\mathbf{s})Q(\mathbf{s}, \mathbf{a})$ from Equation 19, then

- (a) If $\lambda(\mathbf{a}|\mathbf{s}) = h'_f\left(\frac{\pi}{\mu}\right) + \alpha(\mathbf{s}) + \beta(\mathbf{s})Q(\mathbf{s}, \mathbf{a}) > 0$, then $\pi(\mathbf{a}|\mathbf{s})$ is zero due to complementary slackness. Note that $\pi(\mathbf{a}|\mathbf{s}) = 0$, thus $h'_f(0) + \alpha(\mathbf{s}) + \beta(\mathbf{s})Q(\mathbf{s}, \mathbf{a}) > 0$ and we can get $g_f(-\alpha(\mathbf{s}) - \beta(\mathbf{s})Q(\mathbf{s}, \mathbf{a})) < g_f(h'_f(0)) = 0$.
- (b) If $\lambda(\mathbf{a}|\mathbf{s}) = 0$, then $h'_f\left(\frac{\pi}{\mu}\right) + \alpha(\mathbf{s}) + \beta(\mathbf{s})Q(\mathbf{s}, \mathbf{a})$ is zero and $\pi(\mathbf{a}|\mathbf{s}) = \mu(\mathbf{a}|\mathbf{s})g_f(-\alpha(\mathbf{s}) - \beta(\mathbf{s})Q(\mathbf{s}, \mathbf{a})) \geq 0$. Note that $\pi(\mathbf{a}|\mathbf{s}) \geq 0$, thus $h'_f(0) + \alpha(\mathbf{s}) + \beta(\mathbf{s})Q(\mathbf{s}, \mathbf{a}) \leq 0$ and we can get $g_f(-\alpha(\mathbf{s}) - \beta(\mathbf{s})Q(\mathbf{s}, \mathbf{a})) \geq g_f(h'_f(0)) = 0$.

Through analysis (a) and (b), we can resolve optimal policy $\pi^*(\mathbf{a}|\mathbf{s})$ as

$$\pi^*(\mathbf{a}|\mathbf{s}) = \mu(\mathbf{a}|\mathbf{s}) \max \{g_f(-\alpha(\mathbf{s}) - \beta(\mathbf{s})Q(\mathbf{s}, \mathbf{a})), 0\}. \quad (21)$$

Substituting back in Equation 15 and Equation 16 with Equation 8, we can get

$$\mathbb{E}_{\mathbf{a} \sim \mu} [\max \{g_f(-\alpha^*(\mathbf{s}) - \beta^*(\mathbf{s})Q(\mathbf{s}, \mathbf{a})), 0\}] = 1, \quad (22)$$

$$\mathbb{E}_{\mathbf{a} \sim \mu(\mathbf{a}|\mathbf{s})} [Q(\mathbf{s}, \mathbf{a}) \max \{g_f(-\alpha^*(\mathbf{s}) - \beta^*(\mathbf{s})Q(\mathbf{s}, \mathbf{a})), 0\} - V(\mathbf{s})] = 0, \quad (23)$$

□

A.2 Proof of Theorem 3.8

Proof. The Lagrange function of Equation IPF-Soft is written as follows

$$\begin{aligned} L(\pi, \alpha(\mathbf{s}), \beta(\mathbf{s}), \lambda) &= \mathbb{E}_{\mathbf{s} \sim d^\pi(\mathbf{s}), \mathbf{a} \sim \pi(\mathbf{a}|\mathbf{s})} \left[f\left(\frac{\pi(\mathbf{a}|\mathbf{s})}{\mu(\mathbf{a}|\mathbf{s})}\right) + \eta(Q(\mathbf{s}, \mathbf{a}) - V(\mathbf{s}))^2 \right] \\ &\quad - \mathbb{E}_{\mathbf{s} \sim d^\pi(\mathbf{s}), \mathbf{a} \sim \pi(\mathbf{a}|\mathbf{s})} [\lambda(\mathbf{a}|\mathbf{s})\pi(\mathbf{a}|\mathbf{s})] \\ &\quad + \mathbb{E}_{\mathbf{s} \sim d^\pi(\mathbf{s})} \left[\alpha(\mathbf{s}) \left(\int_{\mathbf{a}} \pi(\mathbf{a}|\mathbf{s}) d\mathbf{a} - 1 \right) \right]. \end{aligned} \quad (24)$$

Let $h_f(x) = xf(x)$. Then for all states and actions, the KKT conditions can be written as follows

$$\pi(\mathbf{a}|\mathbf{s}) \geq 0 \quad (25)$$

$$\int_{\mathbf{a}} \pi(\mathbf{a}|\mathbf{s}) d\mathbf{a} = 1 \quad (26)$$

$$\mathbb{E}_{\mathbf{a} \sim \pi(\mathbf{a}|\mathbf{s})} [Q(\mathbf{s}, \mathbf{a}) - V(\mathbf{s})] = 0 \quad (27)$$

$$\lambda(\mathbf{a}|\mathbf{s}) \geq 0 \quad (28)$$

$$\lambda(\mathbf{a}|\mathbf{s})\pi(\mathbf{a}|\mathbf{s}) = 0 \quad (29)$$

$$h'_f\left(\frac{\pi(\mathbf{a}|\mathbf{s})}{\mu(\mathbf{a}|\mathbf{s})}\right) + \alpha(\mathbf{s}) + \eta(Q(\mathbf{s}, \mathbf{a}) - V(\mathbf{s}))^2 - \lambda(\mathbf{a}|\mathbf{s}) = 0 \quad (30)$$

Since h'_f is a strictly increasing function, its inverse function exists and is also a strictly increasing function. Let $g_f = (h'_f)^{-1}(x)$ be its inverse function. From Equation 30, we can get

$$\pi(\mathbf{a}|\mathbf{s}) = \mu(\mathbf{a}|\mathbf{s})g_f\left(\lambda(\mathbf{a}|\mathbf{s}) - \alpha(\mathbf{s}) - \eta(Q(\mathbf{s}, \mathbf{a}) - V(\mathbf{s}))^2\right) \quad (31)$$

Given a state \mathbf{s} , we can get $\lambda(\mathbf{a}|\mathbf{s}) = h'_f\left(\frac{\pi}{\mu}\right) + \alpha(\mathbf{s}) + \eta(Q(\mathbf{s}, \mathbf{a}) - V(\mathbf{s}))^2$ from Equation 30, then

- (a) If $\lambda(\mathbf{a}|\mathbf{s}) = h'_f\left(\frac{\pi}{\mu}\right) + \alpha(\mathbf{s}) + \eta(Q(\mathbf{s}, \mathbf{a}) - V(\mathbf{s}))^2 > 0$, then $\pi(\mathbf{a}|\mathbf{s})$ is zero due to complementary slackness. Note that $\pi(\mathbf{a}|\mathbf{s}) = 0$, thus $h'_f(0) + \alpha(\mathbf{s}) + \eta(Q(\mathbf{s}, \mathbf{a}) - V(\mathbf{s}))^2 > 0$ and we can get $g_f(-\alpha(\mathbf{s}) - \eta(Q(\mathbf{s}, \mathbf{a}) - V(\mathbf{s}))^2) < g_f(h'_f(0)) = 0$.
- (b) If $\lambda(\mathbf{a}|\mathbf{s}) = 0$, then $h'_f\left(\frac{\pi}{\mu}\right) + \alpha(\mathbf{s}) + \eta(Q(\mathbf{s}, \mathbf{a}) - V(\mathbf{s}))^2$ is zero and $\pi(\mathbf{a}|\mathbf{s}) = \mu(\mathbf{a}|\mathbf{s})g_f\left(-\alpha(\mathbf{s}) - \eta(Q(\mathbf{s}, \mathbf{a}) - V(\mathbf{s}))^2\right) \geq 0$. Note that $\pi(\mathbf{a}|\mathbf{s}) \geq 0$, thus $h'_f(0) + \alpha(\mathbf{s}) + \eta(Q(\mathbf{s}, \mathbf{a}) - V(\mathbf{s}))^2 \leq 0$ and we can get $g_f(-\alpha(\mathbf{s}) - \eta(Q(\mathbf{s}, \mathbf{a}) - V(\mathbf{s}))^2) \geq g_f(h'_f(0)) = 0$.

Through analysis (a) and (b), we can resolve optimal policy $\pi^*(\mathbf{a}|\mathbf{s})$ as

$$\pi^*(\mathbf{a}|\mathbf{s}) = \mu(\mathbf{a}|\mathbf{s}) \max\left\{g_f\left(-\alpha(\mathbf{s}) - \eta(Q(\mathbf{s}, \mathbf{a}) - V(\mathbf{s}))^2\right), 0\right\}. \quad (32)$$

let $f(x) = \log x$, then $g_f(x) = \exp(x - 1) > 0$. Substituting back in Equation 32 with $g_f(x) = \exp(x - 1)$, we can get Equation 12. \square

A.3 Proof of Proposition 3.10

Proof. Let $\mathcal{U} = \{\pi(\mathbf{a}|\mathbf{s})|\pi(\mathbf{a}|\mathbf{s}) \geq 0, \int_{\mathbf{a}} \pi(\mathbf{a}|\mathbf{s}) d\mathbf{a} = 1\}$. Since $\inf_{x,y} g(x,y) = \inf_x \inf_y g(x,y)$ and the constraints about π and V in Problem IPF-Soft are independent, we can reformulate Problem IPF-Soft as

$$\begin{aligned} & \min_{\substack{\pi, V \\ s.t. \pi \in \mathcal{U}}} \mathbb{E}_{\mathbf{s} \sim d^\pi(\mathbf{s}), \mathbf{a} \sim \pi(\mathbf{a}|\mathbf{s})} \left[f\left(\frac{\pi(\mathbf{a}|\mathbf{s})}{\mu(\mathbf{a}|\mathbf{s})}\right) + \eta(Q(\mathbf{s}, \mathbf{a}) - V(\mathbf{s}))^2 \right] \\ & = \min_{s.t. \pi \in \mathcal{U}} \min_V \mathbb{E}_{\mathbf{s} \sim d^\pi(\mathbf{s}), \mathbf{a} \sim \pi(\mathbf{a}|\mathbf{s})} \left[f\left(\frac{\pi(\mathbf{a}|\mathbf{s})}{\mu(\mathbf{a}|\mathbf{s})}\right) + \eta(Q(\mathbf{s}, \mathbf{a}) - V(\mathbf{s}))^2 \right]. \end{aligned} \quad (33)$$

For V , this is an unconstrained problem. Setting the gradient with respect to V to 0, we obtain that

$$V(\mathbf{s}) = \mathbb{E}_{\mathbf{a} \sim \pi(\mathbf{a}|\mathbf{s})} [Q(\mathbf{s}, \mathbf{a})]. \quad (34)$$

Substituting back in Equation 33, we can get

$$\begin{aligned} & \min_{s.t. \pi \in \mathcal{U}} \min_V \mathbb{E}_{\mathbf{s} \sim d^\pi(\mathbf{s}), \mathbf{a} \sim \pi(\mathbf{a}|\mathbf{s})} \left[f\left(\frac{\pi(\mathbf{a}|\mathbf{s})}{\mu(\mathbf{a}|\mathbf{s})}\right) + \eta(Q(\mathbf{s}, \mathbf{a}) - V(\mathbf{s}))^2 \right] \\ & = \min_{s.t. \pi \in \mathcal{V}} \mathbb{E}_{\mathbf{s} \sim d^\pi(\mathbf{s}), \mathbf{a} \sim \pi(\mathbf{a}|\mathbf{s})} \left[f\left(\frac{\pi(\mathbf{a}|\mathbf{s})}{\mu(\mathbf{a}|\mathbf{s})}\right) + \eta(Q(\mathbf{s}, \mathbf{a}) - V(\mathbf{s}))^2 \right], \end{aligned} \quad (35)$$

where $\mathcal{V} = \{\pi(\mathbf{a}|\mathbf{s})|\pi(\mathbf{a}|\mathbf{s}) \in \mathcal{U}, V(\mathbf{s}) = \mathbb{E}_{\mathbf{a} \sim \pi(\mathbf{a}|\mathbf{s})} [Q(\mathbf{s}, \mathbf{a})]\}$. Note that \mathcal{V} is the feasible set of Problem IPF.

Since $\inf \{f(x) + g(x)\} \geq \inf f(x) + \inf g(x)$, we can get

$$\begin{aligned} & \min_{s.t. \pi \in \mathcal{V}} \mathbb{E}_{\mathbf{s} \sim d^\pi(\mathbf{s})} \left[f \left(\frac{\pi(\mathbf{a}|\mathbf{s})}{\mu(\mathbf{a}|\mathbf{s})} \right) + \eta (Q(\mathbf{s}, \mathbf{a}) - V(\mathbf{s}))^2 \right] \\ & \geq \min_{s.t. \pi \in \mathcal{V}} \mathbb{E}_{\mathbf{s} \sim d^\pi(\mathbf{s})} \left[f \left(\frac{\pi(\mathbf{a}|\mathbf{s})}{\mu(\mathbf{a}|\mathbf{s})} \right) \right] + \min_{s.t. \pi \in \mathcal{V}} \mathbb{E}_{\mathbf{s} \sim d^\pi(\mathbf{s})} \left[\eta (Q(\mathbf{s}, \mathbf{a}) - V(\mathbf{s}))^2 \right]. \end{aligned} \quad (36)$$

The LHS is exactly Problem IPF, which has the global optimal value at π^*, V^* , so that

$$\begin{aligned} & \min_{s.t. \pi \in \mathcal{V}} \mathbb{E}_{\mathbf{s} \sim d^\pi(\mathbf{s})} \left[f \left(\frac{\pi(\mathbf{a}|\mathbf{s})}{\mu(\mathbf{a}|\mathbf{s})} \right) \right] + \min_{s.t. \pi \in \mathcal{V}} \mathbb{E}_{\mathbf{s} \sim d^\pi(\mathbf{s})} \left[\eta (Q(\mathbf{s}, \mathbf{a}) - V(\mathbf{s}))^2 \right] \\ & \geq p^* + \min_{s.t. \pi \in \mathcal{V}} \mathbb{E}_{\mathbf{s} \sim d^\pi(\mathbf{s})} \left[\eta (Q(\mathbf{s}, \mathbf{a}) - V(\mathbf{s}))^2 \right]. \end{aligned} \quad (37)$$

Let $\mathcal{T} = \{\pi | \pi \in \mathcal{V}, \pi \in \hat{U}(\pi^*, \sigma)\}$, we can get $\mathcal{T} \neq \emptyset$, since \mathcal{V} is a convex set and $\pi^* \in \mathcal{V}$.

Let $k^* = \inf \left\{ \mathbb{E}_{\mathbf{s} \sim d^\pi(\mathbf{s})} \left[(Q(\mathbf{s}, \mathbf{a}) - V(\mathbf{s}))^2 \right] | \pi \in \mathcal{T} \right\}$, we can get $p^* + \eta k^*$ is the minimum value for $\pi \in \mathcal{T}, \forall V$.

Therefore, if the value of Problem IPF at π^*, V^* is less than $p^* + k^*$, then π^*, V^* is a strict local minimizer of Problem IPF. Let $h^* = \mathbb{E}_{\mathbf{a} \sim \pi^*} \left[(Q(\mathbf{s}, \mathbf{a}) - V(\mathbf{s}))^2 \right]$, we can get

$$p^* + \eta h^* < p^* + \eta k^*. \quad (38)$$

So if $\eta(h^* - k^*) < 0$, we can get π^*, V^* is a strict local minimizer of Problem IPF. \square

B Diffusion model

Diffusion Probabilistic Model (DPM). Diffusion models [41, 17, 43] are composed of two processes: the forward diffusion process and the reverse process. In the forward diffusion process, we gradually add Gaussian noise to the data $\mathbf{x}_0 \sim q(\mathbf{x}_0)$ in T steps. The step sizes are controlled by a variance schedule β_i :

$$\begin{aligned} q(\mathbf{x}_{1:T} | \mathbf{x}_0) & := \prod_{i=1}^T q(\mathbf{x}_i | \mathbf{x}_{i-1}), \\ q(\mathbf{x}_i | \mathbf{x}_{i-1}) & := \mathcal{N}(\mathbf{x}_i; \sqrt{1 - \beta_i} \mathbf{x}_{i-1}, \beta_i \mathbf{I}). \end{aligned} \quad (39)$$

In the reverse process, we can recreate the true sample \mathbf{x}_0 through $p(\mathbf{x}^{i-1} | \mathbf{x}^i)$:

$$\begin{aligned} p(\mathbf{x}) & = \int p(\mathbf{x}^{0:T}) d\mathbf{x}^{1:T} \\ & = \int \mathcal{N}(\mathbf{x}^T; \mathbf{0}, \mathbf{I}) \prod_{i=1}^T p(\mathbf{x}^{i-1} | \mathbf{x}^i) d\mathbf{x}^{1:T}. \end{aligned} \quad (40)$$

The training objective is to maximize the ELBO of $\mathbb{E}_{\mathbf{q}_{\mathbf{x}_0}} [\log p(\mathbf{x}_0)]$. Following DDPM [17], we use the simplified surrogate loss

$$\mathcal{L}_d(\theta) = \mathbb{E}_{i \sim [1, T], \epsilon \sim \mathcal{N}(\mathbf{0}, \mathbf{I}), \mathbf{x}_0 \sim q} [|\epsilon - \epsilon_\theta(\mathbf{x}_i, i)|^2] \quad (41)$$

to approximate the ELBO. After training, sampling from the diffusion model is equivalent to running the reverse process.

Conditional DPM. There are two kinds of conditioning methods: classifier-guided [8] and classifier-free [18]. The former requires training a classifier on noisy data \mathbf{x}_i and using gradients $\nabla_{\mathbf{x}} \log f_\phi(\mathbf{y} | \mathbf{x}_i)$ to guide the diffusion sample toward the conditioning information \mathbf{y} . The latter does not train an independent f_ϕ but combines a conditional noise model $\epsilon_\theta(\mathbf{x}_i, i, \mathbf{s})$ and an unconditional model $\epsilon_\theta(\mathbf{x}_i, i)$ for the noise. The perturbed noise $w \epsilon_\theta(\mathbf{x}_i, i) + (w + 1) \epsilon_\theta(\mathbf{x}_i, i, \mathbf{s})$ is used to later generate samples. However [35] shows this combination will degrade the policy performance in offline RL. Following [35, 47] we solely employ a conditional noise model $\epsilon_\theta(\mathbf{x}_i, i, \mathbf{s})$ to construct our noise model ($w = 0$).

Table 3: Hyperparameters for reproducing our results on Table 1.

Dataset	Environment	Learning Rate	η	Reward Tune	Dropout [42]	Expectiles τ	Samples N
Medium-Expert	HalfCheetah	3e-4	-1	Normalization	0.1	0.7	16
Medium-Expert	Hopper	3e-4	-1	Normalization	0.1	0.7	16
Medium-Expert	Walker2d	3e-4	-1	Normalization	0.1	0.7	256
Medium	HalfCheetah	3e-4	-1	Normalization	0.1	0.7	256
Medium	Hopper	3e-4	-1	Normalization	0.1	0.7	64
Medium	Walker2d	3e-4	-1	Normalization	0.1	0.7	256
Medium-Replay	HalfCheetah	3e-4	-1	Normalization	0.1	0.7	64
Medium-Replay	Hopper	3e-4	-1	Normalization	0.1	0.7	256
Medium-Replay	Walker2d	3e-4	-1	Normalization	0.1	0.7	256
Default	AntMaze-umaze	3e-4	1	IQL	0.1	0.9	16
Diverse	AntMaze-umaze	3e-4	1	IQL	0.1	0.9	16
Play	AntMaze-medium	3e-4	-1	IQL	0.1	0.9	64
Diverse	AntMaze-medium	3e-4	-1	IQL	0.1	0.9	16
Play	AntMaze-large	3e-4	1	IQL	0.1	0.9	64
Diverse	AntMaze-large	3e-4	1	IQL	0.1	0.9	64

C Advantage Weighted Regression (AWR)

Prior works [39, 37] formulate offline RL as a constrained policy search (CPS) problem with the following form:

$$\begin{aligned}
 \mu^* &= \arg \max_{\mu} J(\mu) = \arg \max_{\mu} \int_S d_0(\mathbf{s}) \int_{\mathcal{A}} Q^{\mu}(\mathbf{s}, \mathbf{a}) d\mathbf{a} d\mathbf{s} \\
 s.t. \quad &D_{\text{KL}}(\pi_b(\cdot|\mathbf{s})||\mu(\cdot|\mathbf{s})) \leq \epsilon, \quad \forall \mathbf{s} \\
 &\int_{\mathbf{a}} \mu(\mathbf{a}|\mathbf{s}) d\mathbf{a} = 1, \quad \forall \mathbf{s},
 \end{aligned} \tag{42}$$

Previous works [39, 37, 33] solve Equation 42 through KKT conditions and get the optimal policy π^* as:

$$\pi^*(\mathbf{a}|\mathbf{s}) = \frac{1}{Z(\mathbf{s})} \pi_b(\mathbf{a}|\mathbf{s}) \exp(\alpha Q_{\phi}(\mathbf{s}, \mathbf{a})), \tag{43}$$

where $Z(\mathbf{s})$ is the partition function. Intuitively we can use Equation 43 to optimize policy π . However, the behavior policy may be very diverse and hard to model. To avoid modeling the behavior policy, prior works [37, 48, 7] optimize π^* through a parameterized policy π_{θ} , known as AWR:

$$\begin{aligned}
 &\arg \min_{\theta} \mathbb{E}_{\mathbf{s} \sim \mathcal{D}^{\mu}} [D_{\text{KL}}(\pi^*(\cdot|\mathbf{s})||\pi_{\theta}(\cdot|\mathbf{s}))] \\
 &= \arg \max_{\theta} \mathbb{E}_{(\mathbf{s}, \mathbf{a}) \sim \mathcal{D}^{\mu}} \left[\frac{1}{Z(\mathbf{s})} \log \pi_{\theta}(\mathbf{a}|\mathbf{s}) \exp(\alpha Q_{\phi}(\mathbf{s}, \mathbf{a})) \right].
 \end{aligned} \tag{44}$$

where $\exp(\alpha Q_{\phi}(\mathbf{s}, \mathbf{a}))$ being the regression weights. However, AWR requires the exact probability density of policy, which restricts the use of generative models like diffusion models. In this paper, we directly utilize the diffusion-based policy to address Eq. (42). Therefore, our method not only avoids the need for explicit probability densities in AWR but also solves the limited policy expressivity problem.

D Experimental Details

Our implementation is based on IDQL [14] and jaxrl repo which uses the JAX framework to implement RL algorithms. All networks are optimized through the Adam [21]. We clip the multiplier network gradient to prevent gradient explosion due to the exponential term.

D.1 Main Results on D4RL

For the D4RL experiments in Table 1, we only sweep η while keeping other hyperparameters consistent with IDQL to explore the role of alignment. We sweep η since the alignment of policy

depends on the sign of η in different environments. We provide the main hyperparameters in Table 3 to reproduce our results in Table 1. Following IDQL, we use normalization to adjust the rewards, which means $r = r / (r_{\max} - r_{\min})$. For AntMaze tasks, $r = r - 1$.

Networks We follow the [14] to build our policy with an LN_Resnet architecture based conditional diffusion model. To fairly compare our algorithm with IDQL, we use a three-layer network with 256 hidden dim size 256, consistent with IDQL. The critic and value network consistent with IDQL, is a 2 layer MLP with hidden size 256 and ReLU activation function.

We train for 300000 epochs for D4RL tasks with batch size 512, consistent with IDQL. The training curve can be found in Figure 3. We can see due to the policy alignment the training is more stable, even in hard sparse reward tasks like AntMaze large.

LR (For all networks except for multiplier)	3e-4
Critic Batch Size	512
Actor Batch Size	512
τ Expectiles	0.7 (locomotion), 0.9 (AntMaze)
LR	3e-5 for multiplier networks
Grad norm for multiplier on MuJoCo	1.0 (α), 0.5 (β)
Grad norm for multiplier on AntMaze	1.0 (α), 1 (β)
Critic Grad Steps	3e6
Actor Grad Steps	3e6
Target Critic EMA	0.005
T	5
Beta schedule	Variance Preserving [44]
Actor Dropout Rate	0.1 for actor on all tasks
Critic Dropout Rate	0.1 for AntMaze Tasks in AlignIQL-hard
Number Residual Blocks	3
Actor Cosine Decay [29]	Number of Actor Grad Steps
Optimizer	Adam [21]

D.2 Sparse Rewards Tasks

For sparse reward tasks, we use $\eta = 1 > 0$ and $\tau = 0.7$ and keep other hyperparameters the same as Table 3. The weight of IDQL is $w_2^\tau(s, a) = |\tau - \mathbb{1}(Q(s, a) < V_\tau^2(s))|$. since we use expectile regression to train the critic. We also follow the IDQL’s advice the take the max probability action at evaluation time.

D.3 Results of AlignIQL-hard

In this chapter, we report the results of AlignIQL-hard. Table D.1 reports the hyperparameters we used for AlignIQL-hard.

Table 4: Average Results of AlignIQL-hard on D4RL tasks.

D4RL Tasks	AlignIQL-hard			AlignIQL		
	$N = 16$	$N = 64$	$N = 256$	$N = 16$	$N = 64$	$N = 256$
Locomotion	69.7	71.0	71.5	73.2	74.0	72.3
AntMaze	54.2	57.9	56.7	65.8	70.2	70.7

We also report the performance of AlignIQL under different N . For the MuJoCo tasks, we report the results for $\eta = -1$, and for AntMaze, we report the results for $\eta = 1$. Therefore, the results in Table 4 are slightly lower than those in Table 1. For AlignIQL and AlignIQL-hard, especially

for AlignIQL-hard, we perform minimal hyperparameter tuning. In most cases, we use the default parameters of IDQL. Therefore, the performance of our algorithm can be further improved with additional tuning.

E Training Curves D4RL Tasks

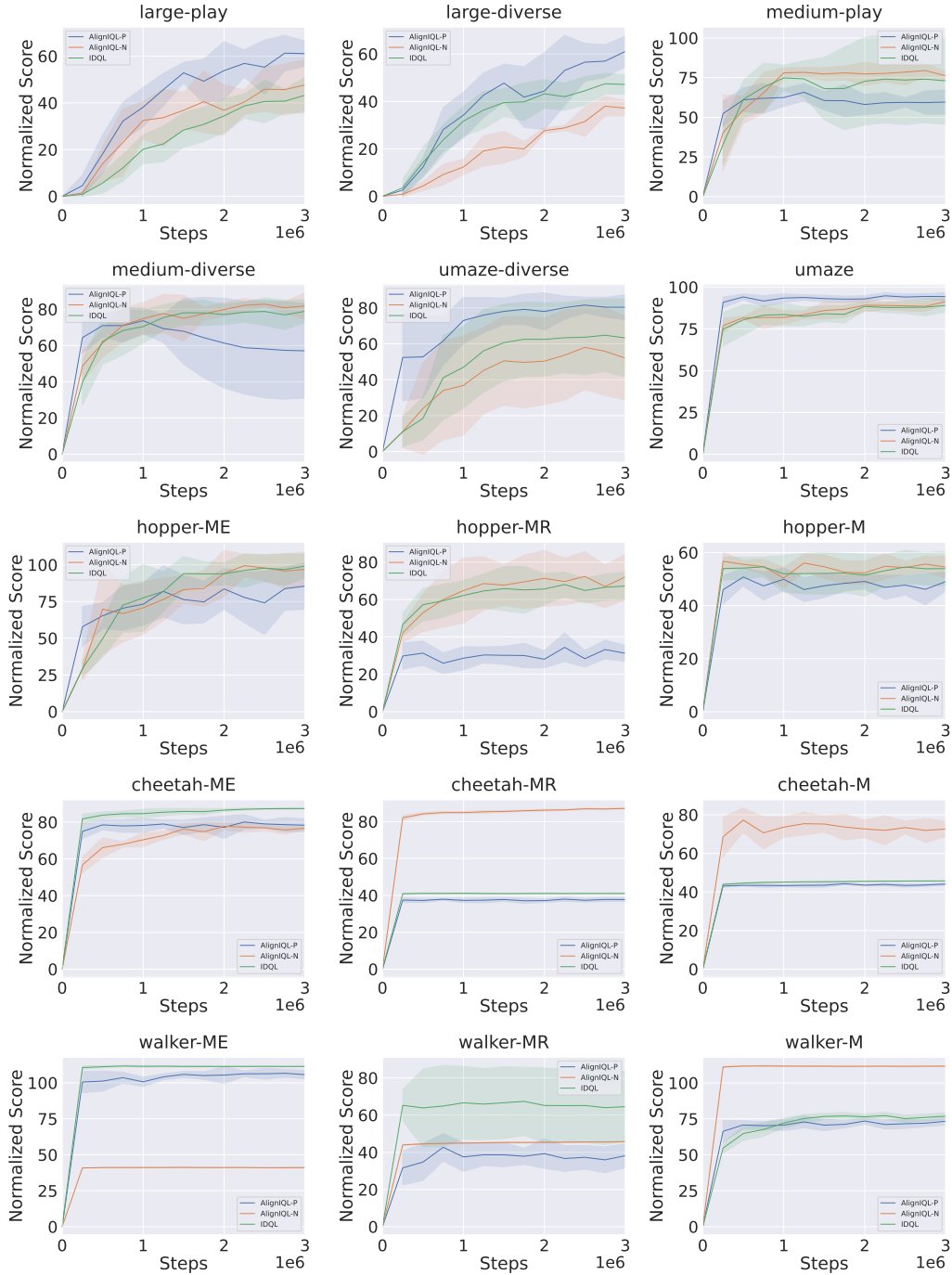


Figure 3: Training curves of AlignIQL and IDQL, where AlignIQL-P means we use hyperparameter $\eta > 0$ and AlignIQL-N means $\eta < 0$. The normalized score is calculated by averaging the scores for the three different N ($N = 16, 64, 256$), where N represents the number of actions generated by the diffusion-based behavior policy.